

Lattice Matching and Thermal Expansion in the Pb-Sn-Te System

Lead tin telluride in the form of LPE-grown multilayered structures is a semiconducting material used in opto-electronic devices. In the case of laser diodes, special attention is paid to reduce the threshold current density, J_{th} , to permit cw operation at relatively high temperatures. In the III-V system, the use of a double heterostructure (DH) configuration has resulted in a remarkable improvement in the performance of the prepared lasers, compared with that of lasers prepared from homostructures (e.g., Ref. 1). Similar improvements were expected for the PbSnTe DH lasers; however, the performance of PbSnTe DH lasers did not differ significantly from the homostructure analog (2, 3). This was explained by the high dislocation densities at the heterointerfaces, which probably act as nonradiative recombination centers increasing J_{th} significantly (4). The main source of the dislocations at the heterointerface is the lattice mismatch, Δa , of the adjacent crystals at the heteroboundary (5, 6) at growth temperature (7), provided the thermal expansion coefficients of layer and substrate are similar. Otherwise, on cooling, postgrowth stress due to the difference in the thermal expansion coefficients results in an additional generation of dislocations.

Recently, room-temperature lattice-matched heterostructures of $PbTe_{1-y}Se_y/Pb_{1-x}Sn_xTe$ ($x = 0.21$, $y = 0.08$) lasers were fabricated (8). However, these lasers still operate at low temperatures with higher J_{th} than lasers prepared from homostructures (9). This was also attributed to higher structural defects at the PbTeSe/PbSnTe heteroboundary than at the homostructure bound-

ary. The most important aspect of lattice parameter control and generation of misfit dislocations is the fine adjustment of the layer-substrate misfit at the growth temperature. However, the lattice constants of $Pb_{1-x}Sn_xTe$ ($0 \leq x \leq 1$) and $PbTe_{1-y}Se_y$ ($0 \leq y \leq 1$) alloys were measured only at room temperature (10) and the thermal expansion coefficients of these alloy systems are unknown.

In the present study, accurate measurements of the lattice constants of several $Pb_{1-x}Sn_xTe$ and $PbTe_{1-y}Se_y$ alloy compositions were carried out in the temperature range 25–600°C. Special attention was paid to the common LPE growth temperature range, 400–600°C, and the compositions x and y used in laser fabrication.

Polycrystalline $Pb_{1-x}Sn_xTe$ ($0 \leq x \leq 1$) and PbSe were prepared directly from the elements, and $PbTe_{1-y}Se_y$ ($y = 0.08$) samples were prepared from the appropriate amounts of PbTe and PbSe. The materials were of 6N grade, with Pb and Sn etched before use. The stoichiometric charges were sealed under high vacuum ($\sim 10^{-7}$ Torr) in a cleaned quartz ampoule, heated to 1000°C in a rocking furnace for ~ 20 hr, and then quenched in a water bath. After grinding the polycrystalline material into a fine powder, further annealing was carried out at 350°C, under high vacuum, for about 4 days. The samples were furnace-cooled to room temperature.

The Bragg angles of the (6,2,0), (6,2,2), (6,4,0), and (6,4,2) reflections of the samples were measured by a vertical Philips powder diffractometer using a Cu target. A PW 1158 high-temperature attachment was used to obtain powder patterns at elevated

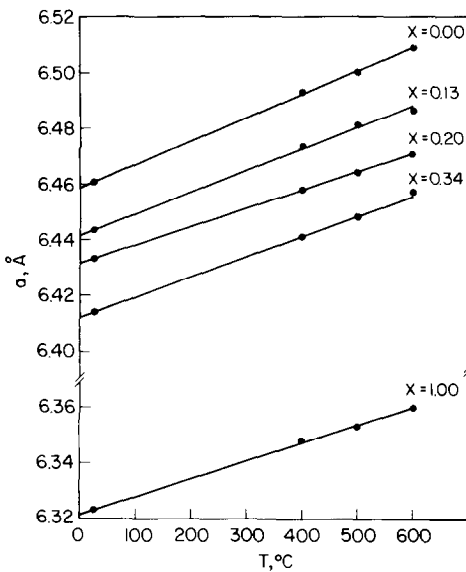


FIG. 1. Lattice constants, a , of the $\text{Pb}_{1-x}\text{Sn}_x\text{Te}$ system for various x values as a function of temperature.

temperatures. The sample, held in a tungsten boat, was placed in a slot on a tungsten sample holder. The diffraction lines were measured at 20, 400, 500, 600, and again at 20°C, under constant pumping, the vacuum in the sample chamber being $\sim 10^{-5}$ Torr. The sample temperature was monitored by a suitable thermocouple ($\pm 5^\circ\text{C}$). The scanning rate was $0.125^\circ/\text{min}$, with an accuracy of $\pm 0.02^\circ$ in the determination of the diffraction angles.

No phase changes were observed in the polycrystalline samples of $\text{Pb}_{1-x}\text{Sn}_x\text{Te}$ ($0 \leq x \leq 1$), PbSe , and $\text{PbTe}_{0.92}\text{Se}_{0.08}$ on heating, up to 600°C . The diffraction patterns of the samples taken at room temperature before and after heating showed identical reflections. Hence no material decomposition occurs during the prolonged (~ 10 hr) heat treatment of the samples under constant pumping.

Figure 1 shows the variation of the lattice parameters of the $\text{Pb}_{1-x}\text{Sn}_x\text{Te}$ ($0 \leq x \leq 1$) alloys with temperature. The straight lines demonstrate a constant thermal coefficient of expansion over the temperature range in-

vestigated. Therefore, the lattice parameter of any composition x in the $\text{Pb}_{1-x}\text{Sn}_x\text{Te}$ system can be calculated for a given temperature from the relation

$$a_T = a_0(1 + \alpha T), \quad (1)$$

where α = thermal expansion coefficient, a_0 = lattice parameter at 0°C , and a_T = lattice parameter at temperature T . The α and a_0 values for any composition x in the $\text{Pb}_{1-x}\text{Sn}_x\text{Te}$ system are given in Fig. 2; α can be taken as a linear, inversely proportional function of x . The difference in lattice parameters of any two given $\text{Pb}_{1-x}\text{Sn}_x\text{Te}$ crystals with different composition x decreases with decreasing T .

Although the lattice parameters of the samples at various T were determined for polycrystalline powders, it is assumed that these values represent the lattice param-

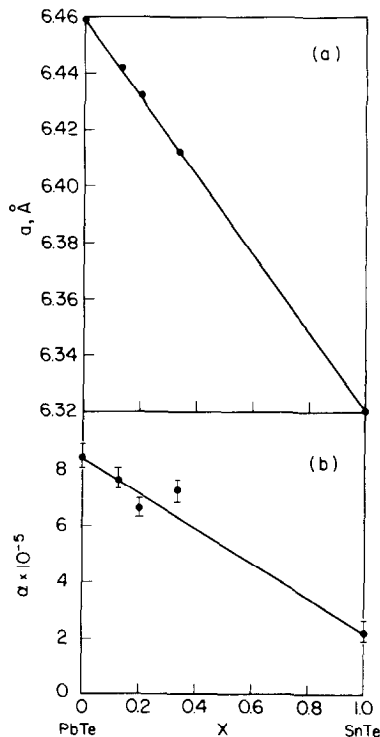


FIG. 2. (a) Lattice parameter at 0°C , a_0 , and (b) thermal expansion coefficient α for the $\text{Pb}_{1-x}\text{Sn}_x\text{Te}$ alloy system.

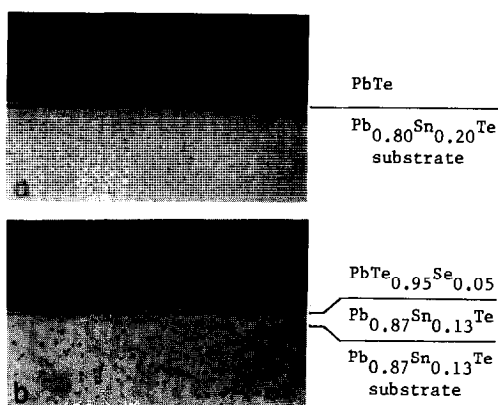


FIG. 3. Cleaved and etched cross sections of (a) 4- μm -thick PbTe epilayer on $\text{Pb}_{0.80}\text{Sn}_{0.20}\text{Te}$ substrate, $\Delta a/a$ (25°C) = 4.26×10^{-3} ; (b) room-temperature lattice-matched 4- μm -thick $\text{PbTe}_{0.95}\text{Se}_{0.05}$ epilayer, on 7- μm -thick $\text{Pb}_{0.87}\text{Sn}_{0.13}\text{Te}$ epilayer grown on $\text{Pb}_{0.87}\text{Sn}_{0.13}\text{Te}$ substrate ($\times 260$).

ters of any grown epilayer with the same composition x , provided the epilayer thickness, d , is high enough. For the GaAlAs system, the layer thickness threshold, d_{th} , in which the misfit strain is relieved by generation of misfit dislocations is known to be about 1–2 μm (11). Since the lattice mismatch at the LPE growth temperatures of PbTe/SnTe is 2.30×10^{-2} compared with 1.41×10^{-4} for GaAs/AlAs, it is reasonable to assume that for the PbSnTe system $d_{\text{th}} < 1 \mu\text{m}$. Any $\text{Pb}_{1-x}\text{Sn}_x\text{Te}$ grown epilayer with $d > 1 \mu\text{m}$ will have a lattice parameter similar to that of any bulk crystal or polycrystalline powder of the same composition x . Therefore, the lattice mismatch between any two adjacent epilayers in PbSnTe heterostructures can be determined from the lattice parameters measured in the present work, for any temperature between 25–600°C and any composition x .

In order to study the effect of lattice mismatch on the interface quality in the PbSnTe system, three types of epilayer structures were grown: (I) lattice-mismatched heterostructures, (II) homostructures, and (III) room-temperature lat-

tice-matched heterostructures. The experimental details of epilayer growth were described previously (12). Examples of cleaved and etched (6) cross sections of each type are shown in Fig. 3: type (I) PbTe epilayer grown on $\text{Pb}_{0.80}\text{Sn}_{0.20}\text{Te}$ substrate, type (II) $\text{Pb}_{0.87}\text{Sn}_{0.13}\text{Te}$ epilayer grown on $\text{Pb}_{0.87}\text{Sn}_{0.13}\text{Te}$ substrate, together with type (III) $\text{PbTe}_{0.95}\text{Se}_{0.05}$ epilayer grown on $\text{Pb}_{0.87}\text{Sn}_{0.13}\text{Te}$. The homointerface (type (II)) cannot be detected. However, the heterointerfaces are clearly observed because of the line of successive etch pit (misfit) dislocations at the heteroboundary. While the PbTe/ $\text{Pb}_{0.80}\text{Sn}_{0.20}\text{Te}$ interface is relatively rough and broad, the $\text{PbTe}_{0.95}\text{Se}_{0.05}$ / $\text{Pb}_{0.87}\text{Sn}_{0.13}\text{Te}$ is quite flat and narrow.

An example of a change in lattice parameters of room-temperature lattice-matched materials $\text{PbTe}_{0.92}\text{Se}_{0.08}$ and $\text{Pb}_{0.80}\text{Sn}_{0.20}\text{Te}$ as a function of temperature is given in Fig. 4. A difference in the lattice parameters develops with increasing temperature, reach-

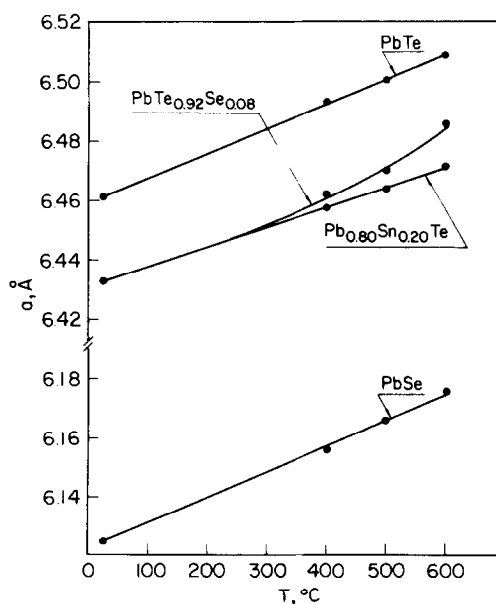


FIG. 4. Lattice constants, a , of PbTe, PbSe, and room-temperature lattice-matched $\text{PbTe}_{0.92}\text{Se}_{0.08}$ and $\text{Pb}_{0.80}\text{Sn}_{0.20}\text{Te}$, as a function of temperature.

ing a value of $\Delta a/a = 2.38 \times 10^{-3}$ at 600°C. The two materials have different α values, with a nonlinear behavior of α with T for the selenide case. The improved interface quality of the $\text{PbTe}_{0.92}\text{Se}_{0.08}/\text{Pb}_{0.80}\text{Sn}_{0.20}\text{Te}$ structure compared with the $\text{PbTe}/\text{Pb}_{0.80}\text{Sn}_{0.20}\text{Te}$ structure is a result of the lower lattice mismatch at the LPE growth temperature, ~500°C: in the former $\Delta a/a = 1 \times 10^{-3}$, while in the latter $\Delta a/a = 5.63 \times 10^{-3}$. However, the misfit dislocations of the $\text{PbTe}_{0.92}\text{Se}_{0.08}/\text{Pb}_{0.80}\text{Sn}_{0.20}\text{Te}$ system formed at epilayer growth do not disappear on cooling, although lattice matching exists at room temperature. Hence the difference in thermal expansion coefficients of the adjacent materials in the heterostructure explains why introducing the selenide component (8) in order to obtain a room-temperature lattice-matched heterostructure could not lead to a DH laser diode with high-quality performance, as reported for the AlGaAs system.

References

1. M. B. PANISH, I. HAYASHI, AND S. SUMSKI, *Appl. Phys. Lett.* **16**, 326 (1970).
2. S. H. GROOVES, K. W. NILL, AND A. J. STRAUSS, *Appl. Phys. Lett.* **25**, 331 (1974).

3. W. LO, *J. Quant. Electron.* **QE-13**, 591 (1977).
4. D. KASEMSET AND C. G. FONSTAD, *Appl. Phys. Lett.* **34**, 432 (1979).
5. N. TAMARI AND H. SHTRIKMAN, *J. Appl. Phys.* **50**, 5736 (1979).
6. M. YOSHIKAWA, M. ITO, K. SHINOHARA, AND R. UDEA, *J. Cryst. Growth* **47**, 230 (1979).
7. G. A. ROZGONYI, P. M. PETROFF, AND M. B. PANISH, *J. Cryst. Growth* **27**, 106 (1974).
8. D. KASEMSET, S. ROTTER, AND C. G. FONSTAD, *IEEE Electron Device Lett.* **EDL-1**, 75 (1980).
9. M. ORON, Ph.D. thesis, submitted to Tel-Aviv University (1981), and private communication.
10. N. R. SHORT, *Brit. J. Appl. Phys.* **1**, 129 (1968).
11. P. M. PETROFF, G. A. ROZGONYI, AND M. B. PANISH, presented at 4th International Conference on Crystal Growth, Tokyo, 1974.
12. Y. STERNBERG AND N. YELLIN, *J. Cryst. Growth* **53**, 535 (1981).

Y. STERNBERG*
 N. YELLIN*†
 S. COHEN‡
 L. BEN DOR‡

* Soreq Nuclear Research Centre, Yavne, Israel

‡ The Hebrew University, Jerusalem, Israel

Received February 19, 1982

† Correspondence should be addressed to N. Yellin.